Mon. Not. R. astr. Soc. (1980) **192**, 321–337

Two-dimensional simulation of the gravitational system dynamics and formation of the large-scale structure of the Universe

A. G. Doroshkevich, E. V. Kotok, I. D. Novikov*, A. N. Polyudov, S. F. Shandarin and Yu. S. Sigov

Institute of Applied Mathematics, Academy of Science, Miusskaja Pl., 4, Moscow 125047, USSR

Received 1979 September 28; in original form 1979 February 12

Summary. The results of a numerical experiment are given that describe the non-linear stages of the development of perturbations in gravitating matter density in the expanding Universe. This process simulates the formation of the large-scale structure of the Universe from an initially almost homogeneous medium. In the one- and two-dimensional cases of this numerical experiment the evolution of the system from 4096 point masses that interact gravitationally only was studied with periodic boundary conditions (simulation of the infinite space). The initial conditions were chosen that resulted from the theory of the evolution of small perturbations in the expanding Universe. The results of numerical experiments are systematically compared with the approximate analytic theory.

The results of the calculations show that in the case of collisionless particles, as well as in the gas-dynamic case, the cellular structure appeared at the non-linear stage (when $\delta\rho/\rho \gtrsim 1$) in the case of the adiabatic perturbations. The greater part of the matter is in thin layers that separate vast regions of low density. In a Robertson–Walker universe ($\Omega = 1$) the cellular structure exists for a finite time and then fragments into a few compact objects. In the open Universe ($\Omega < 1$) the cellular structure also exists if the amplitude of initial perturbations is large enough. But the following disruption of the cellular structure is more difficult because of too rapid an expansion of the Universe. The large-scale structure is frozen. Formation of the cellular structure depends mainly on the choice of the spectrum of initial perturbations (short waves must be suppressed).

1 Introduction

When a theory of galaxy formation is developed (Zeldovich & Novikov 1975) we are inevitably faced with the necessity of studying complex motions of matter in conditions where gravitational forces are a significant, if not decisive, factor. This is true about the

* Institute of Space Research, Academy of Science, Profsoyuznaja, 84/32, Moscow 117810, USSR.

problems in the non-linear theory of gravitational instability, those of violent relaxation and evolution in systems of gravitationally interacting point masses, and about many other problems of the same kind. They have much in common with a broad range of problems related to plasmas; hence they can be analysed with the help of numerical methods worked out for the solution of multidimensional plasma problems (Kotok & Sigov 1970).

The paper deals with the analysis of the problems of small, long-wave perturbations evolving at a non-linear stage under the effect of gravitational forces. The problem is closely linked with the theory of galaxy formation from acoustic perturbations. Here we do not consider the entropy theory of galaxy formation.

The origin of galaxies, according to the theory can be generally described as follows. At early stages in the evolution of the hot Universe there occurred slight deviations from homogeneity and isotropy in the expanding, almost homogeneous, mixture of ionized matter and radiation. This period of small perturbation evolution has been analysed analytically (Lifshitz 1946; Zeldovich & Novikov 1975). It turns out that during the expansion only certain long-wave acoustic perturbations of density are maintained and potential motion velocities, associated with them. All other motions as well as short-wave acoustic oscillations will be attenuated. At some instant in time the cooling, expanding plasma is rapidly neutralized, and the pressure of the matter, within the scales we are interested in, turns out to be negligible compared with gravitational forces. An approximate solution of the non-linear stage of the evolution of perturbations under the conditions mentioned is given by Zeldovich (1970). He has shown that evolution of small perturbations, in the conditions when the effect of pressure on the motion of the matter can be neglected, brings about an extremely particular picture. The matter disintegrates into thin, dense formations – 'pancakes' – which have (in the limit of negligible entropy) infinite density, with the surface density being finite (see also Novikov 1975). It is assumed that with time, disintegration of these 'pancakes' into smaller parts and their clustering could result in the non-uniform distribution of galaxies and their clusters in space, which we now observe. Whether the approximate theory is well-substantiated and accurate has been checked by various analytical (indirect) and numerical methods and it was recognized to be satisfactory (Doroshkevich, Ryabenki & Shandarin 1973).

This approximate theory, however, can only be applied with many restrictions and in no case is acceptable after regions of infinite density appear, that is, for the analysis of further evolution of 'pancakes'. Such an analysis as well as detailed comparison of the rigorous and approximate theories require a numerical experiment to be carried out.

The paper presents the results of a numerical simulation of the process of 'pancake' formation and evolution in the case of collisionless particles, including the stage at which the approximate theory does not obviously hold. The results of comparison of the approximate theory with the numerical experiment is also given.

Of course, formation and subsequent evolution of 'pancakes' in the case of collisionless particles is not the same as the gas-dynamic theory of 'pancakes' that is the basis of the adiabatic theory of galaxy formation, where dissipation is essential. However, the results of our numerical simulations have shown that in the case under consideration the resultant large-scale picture has general similarity to the gas-dynamic picture: the formed cellular structure being seen clearly (see Section 3). In the open Universe ($\Omega < 1$) the cellular structure is frozen but if $\Omega \geqslant 1$ it will evolve, forming distinct clouds.

Considering the dissipationless evolution of perturbations of density enables one to clarify the effect of dissipation on the process of galaxy formation in the adiabatic theory. Besides, the problem has its own significance because it can describe formation of the large-scale structure in some variant of the entropy theory.

The idea of a numerical experiment was to solve one- and two-dimensional problems using a program of two-dimensional simulation, developed to study the evolution of a system of point masses interacting according to Newton's law. For this purpose well-developed methods of discrete modelling of plasma are used (Hockney 1970). The Vlasov kinetic equation for gravitating particles is numerically solved by means of the 'cloud in cell' method (Birdsull 1969). The Poisson equation is solved by the method of establishment (Samarsky 1971; Fedorenko 1973). In our simulations, the parameters of the system are: number of particles = 4096; spatial region was a square with dimensions $2\pi \times 2\pi$; number of 'cells' = 64×64; a 'particle' was a square with dimension $2\pi/64$; the boundary conditions were periodic.

The equations of growth of perturbations in the expanding Universe are developed in Section 2. Evolution of the one-dimensional perturbation in the collisionless self-gravitating system is considered in Section 3. In Section 4 results of the numerical simulations of two-dimensional systems are given.

2 Transformation of equations

The far-reaching analogy between gravitational and electromagnetic interactions is widely used in the analysis of evolution of gravitating particle systems. The major difference between gravity and electromagnetism is the absence of gravitational repulsion (unless hypothetical negative mass is introduced). Hence, the system of gravitating particles always has a positive total mass, which is contrary to the plasma where systems are assumed to have a zero net charge. Hence stationary gravitating systems are either non-uniform or gravitational interaction within them is balanced by external forces.

The situation is different in the case of the evolution of a non-stationary quasi-uniform gravitating medium, the expansion of which obeys Hubble's law, the situation analysed in the present paper. In this case the general Hubble's expansion effectively compensates gravitational attraction, and the problems of the development of inhomogeneities superposed upon the gravitating medium turn out to be very similar (in terms of the formalism used) to those of the evolution of a quasi-homogeneous plasma.

This was shown (Doroshkevich *et al.* 1973; Doroshkevich & Shandarin 1973) with hydrodynamic equations as an example. The same is shown here for a more general case of Vlasov's equation for a gravitating medium. As is known (Polyachenko & Friedman 1976), the evolution of a system of particles which only interact gravitationally is described by Vlasov's equation:

$$\frac{\partial f}{\partial t} + v_i \frac{\partial f}{\partial x_i} + F_i \frac{\partial f}{\partial u_i} = 0,$$
$$\frac{\partial F_i}{\partial x_i} = -4\pi G\rho \equiv -4\pi G \int f d^3 v, \tag{1}$$

where $f = f(t, x_i, v_i)$ is the one-particle distribution function, t is the time, x_i the coordinate, v_i the velocity of a particle, F_i the gravitational force acting upon the particle, ρ the density and G is the Newton gravity constant.

If the evolution of inhomogeneities is considered against the background of the expanding matter then it is convenient to distinguish the uniform background and change over to values:

$$x_i' = (1+z)x_i; \quad v_i' = (1+z)^{-1}(v_i - Hx_i); \quad \rho' = (1+z)^{-3}\rho;$$
$$t' = -\int_t^\infty (1+z)^2 dt = \frac{2}{\Omega H_0}(\sqrt{1-\Omega} - \sqrt{1+\Omega z}), \tag{2}$$

here z is the redshift, so $(1+z)^{-1}$ is proportional to the expansion factor, H is the Hubble constant, H_0 the present Hubble constant and $\Omega = 8\pi G\bar{\rho}_0/3H_0^2$ the dimensionless density at the present time. In the integral (2) the usual relation between time t and redshift z is used. In equation (2) it is assumed that $\Omega \leqslant 1$, the similar formula for $\Omega > 1$ is evident.

The substitution of variables (2) into Vlasov's equation (1) yields in the primed variables

$$\frac{\partial f'}{\partial t'} + v_i' \frac{\partial f'}{\partial x_i'} + F_i' \frac{\partial f'}{\partial v_i'} = 0,$$

$$F_i' = (1+z)^{-3}\left(F_i + \frac{4\pi G}{3}\bar{\rho}x_i'\right), \tag{3}$$

$$\frac{\partial F_i'}{\partial x_i'} = -4\pi G(1+z)^{-1}[\rho' - (1+z)^{-3}\bar{\rho}] = -4\pi G'\left(\int f' d^3v' - \bar{\rho}_0\right).$$

Equations (3) coincide with equation (1) with an accuracy of the gravity constant G being replaced by $G' = G(1+z)^{-1}$ and the redefinition of density. Together with this the condition of 'electrical neutrality' is met in equation (3) since the density is now described by $\rho' = (1+z)^{-3}\bar{\rho}$, and the integral of density over the entire space is obviously equal to zero, because of the conservation of mass. Hence, the problems of evolution of the system of gravitating masses in primed coordinates can be solved with the help of numerical methods used in the theory of plasmas.

Gravitational problems have some specific features, compared with the plasma theory, that become evident from equation (3). First, due to the non-linear transformation of time, it is the increase of the interaction constant $G' = G(1+z)^{-1}$ with time t' (parameter z decreases with growing time t') which results in stronger interaction in the system. Secondly it should be mentioned that the 'gravitational neutrality' of the system is only the average taken over the whole system. The 'negative' density of the charge, given by the term $-(1+z)^{-3}\bar{\rho} = -\bar{\rho}_0$ is strictly constant over space and constant over time, while the 'positive' charge density, ρ', generally has an extremely inhomogeneous distribution. In the region with condensations of material points $\rho' \gg \bar{\rho}_0$, while in the region with rarefactions $\rho' \ll \bar{\rho}_0$. In the gravitational field, charges of the same sign attract each other which causes the well-known gravitational instability.

Equation (3) can be instrumental in the calculation by conventional means, the law of energy conservation in the system. Taking into account the time dependence of the modified gravity 'constant' G', we obtain

$$\frac{dT'}{dt'} = \frac{dU'}{dt'} - H'U' \tag{4}$$

where

$$T' = \tfrac{1}{2}\int v'^2 f'\, d^3v'\, d^3x'; \qquad U' = \tfrac{1}{2}\int(\bar{\rho}' - \bar{\rho}_0)\phi'\, d^3x'$$

$$\frac{\partial^2\phi'}{\partial x_i'^2} = 4\pi G'(\rho' - \bar{\rho}_0); \qquad H' = -\frac{d\ln(1+z)}{dt'}.$$

The time dependence of $G' = G(1+z)^{-1}$ has brought about the term $-H'U'$ in equation (4). Equation (4) is identical to the Irvine–Dmitriev theorem (Irvine 1961; Dmitriev & Zeldovich 1963, 1964).

To conclude this section we would like to mention that the substitution to the plasma primed coordinates is valid not only for Vlasov's equation but also for the most general case

of the system of gravitationally interacting particles, that expands according to Hubble's law. In all the above transformations no conditions were imposed on the function f. Hence, the transition of (1–3) – type is also valid for n-particle distribution function and for Liouville's equation.

3 Analysis of a one-dimensional problem

Equation (3) is significantly simplified so that the evolution of inhomogeneities on a much larger scale can be studied such that the effect of matter, temperature and pressure on the evolution can be neglected until there appear condensations with a high (infinite in the limit) density. Neglecting the pressure, we may turn from system (3) to the set of equations for density and mean velocity. In this approximation we have

$$\begin{aligned}
&\frac{\partial \rho'}{\partial t'} + \frac{\partial}{\partial x'_i}(\rho' v'_i) = 0,\\
&\frac{\partial v'_i}{\partial t'} + v'_k \frac{\partial v'_i}{\partial x'_k} = F'_i,\\
&\frac{\partial F'_i}{\partial x'_i} = -4\pi G'(\rho' - \bar{\rho}_0).
\end{aligned} \tag{5}$$

The system (5) is solved analytically for one-dimensional inhomogeneities, i.e. for $v'_2 \equiv v'_3 \equiv 0; F'_2 \equiv F'_3 \equiv 0; \rho' = \rho'(t', x'_1)$.

In this case (Sunyaev & Zeldovich 1972)

$$\begin{aligned}
&x'_1 = q_1 - B(t') \cdot s_1(q_1),\\
&v'_1 = -\frac{dB}{dt'} \cdot s_1(q_1),\\
&\rho' = \bar{\rho}_0 \left(1 - B(t') \cdot \frac{ds_1}{dq_1}\right)^{-1}
\end{aligned} \tag{6}$$

where $s_1(q_1)$ is the particle displacement from the unperturbed position and the $B(t')$ function is determined by the following equation:

$$\begin{aligned}
&\frac{d^2 B}{dt'^2} = 4\pi G' \bar{\rho}_0 B,\\
&B = 4H_0^{-2}(t')^{-2} \qquad \text{for} \qquad \Omega = 1.
\end{aligned} \tag{7}$$

The solution in equation (6) holds until peculiarities appear in ρ' (at the point where $\lambda_1 = ds_1/dq_1 > 0$ and has a maximum in the region discussed).

If the problem is to be solved in the hydrodynamical approximation (Zeldovich 1970; Zeldovich & Novikov 1975), it can be shown that the solution (6) is no longer valid after the intersection of particles. A shock-wave has formed and stopped and heated up the following matter to a high temperature. A detailed analysis of the problem is given in Doroshkevich & Shandarin (1973), Sunyaev & Zeldovich (1972) and Zeldovich & Novikov (1975).

If the evolution of the collision-free system of gravitationally interacting point masses is studied, then, even at a later stage, the appearance (formal) of a singularity in the density

in the case of one-dimensional contraction does not prevent the study of the evolution of such a system. It is clear that the analytical solution (6) no longer holds here and the computer numerical procedure has been used in the analysis.

As was mentioned by Zeldovich (1970) gravitational potential as well as gravitational force remains regular during the one-dimensional collapse despite singularity. This reason lowers the requirements on the accuracy of the calculation of motion of particles near a singular point and gives a possibility for a rather good description of small-scale structure of a 'pancake' in the numerical simulations.

As an example, we investigate the evolution of a system of gravitationally interacting point masses, with the initial displacement in equation (6) taken as:

$$s_1(q_1) = -A_1 \sin q_1 \tag{8}$$

in the square with $0 \leqslant q_1 \leqslant 2\pi$, $0 \leqslant q_2 \leqslant 2\pi$ with periodical boundary conditions. A similar case was also discussed by Sunyaev & Zeldovich (1972). In this case, as equation (6) shows, particles are focused in the point $q_1 = \pi$ at time t'_f determined by the condition:

$$A_1 B(t'_f) = 1. \tag{9}$$

If the dimensionless mean density is assumed to be $\Omega = 1$, then according to equations (2), (7) and (9) the instant of time when the focusing occurs

$$t'_f = -\frac{2\sqrt{A_1}}{H_0} \tag{10}$$

is determined by setting the values of perturbation amplitudes (for fixed H_0). No doubt the selection of the amplitude, A, and H_0 only determines the scale of t'_f. In fact, after the displacement profile $s_1(q_1)$ is selected, the problem does not depend any longer on any constants or functions. Because of this, the time for the beginning of the numerical calculation is, in effect, not important in a strictly one-dimensional problem (it is only required that it precedes the moment of focusing). The beginning can be varied to test the accuracy of the numerical calculations. It should be mentioned that out of the two linearly independent solutions of equation (7) only the increasing one is taken. The choice of only this mode corresponds to the physical statement of the problem of showing how galaxies form in the expanding Universe. (For more detail see Zeldovich & Novikov 1975.) Below we shall discuss only increasing modes. At the moment when focusing occurs the wave 'breaks' down; the derivative

$$\frac{\partial v'_1}{\partial x'_1} = -\frac{dB}{dt'} \cdot \frac{ds_1}{dq_1} \left(1 - B\frac{ds_1}{dq_1}\right)^{-1} \tag{11}$$

becomes infinite in the point $q_1 = \pi$. In the next moment first particles fly over the plane of symmetry $x_1 = \pi$, thus bringing about multistream motion.

The problem is very similar to the well-known problems of simple waves breaking in a non-dispersive medium (Kadomzev 1976). The difference is that the evolution of the system is considered, with the gravitational interaction taken into account, which is prominent after the wave has broken down. Before it the gravity only affects the shape of the function $B(t')$. Besides, we study the evolution of the system over a spatial scale equal to one wavelength. In the problem under consideration the pressure of the medium is neglected; that is equivalent to the assumption of the absence of dispersion in the medium. The effect of pressure on the wave breaking down was discussed by Shukurov (1979).

The evolution of the system after the focusing is, in fact, determined by gravitation. As has been mentioned above, the period was studied by the methods of numerical simulation.

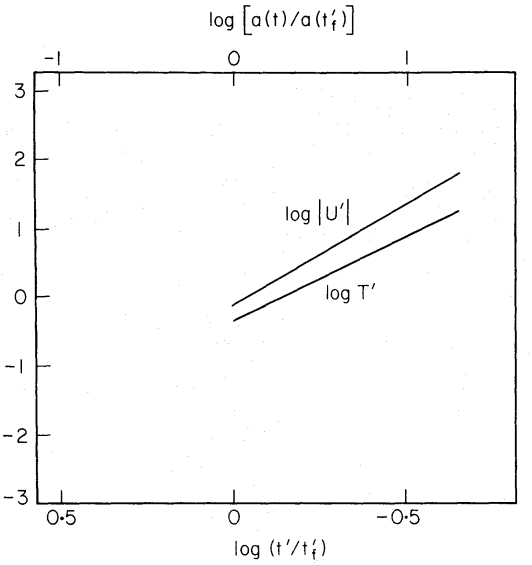

Figure 1. Dependence of kinetic T' and potential U' energies on time in the one-dimensional problem. The displacement is chosen as $s_1(q_1) = -A_1 \sin(q_1)$. Before focusing $|U'| \sim T' \sim |t'|^{-6}$ after focusing $|U'| \sim |t'|^{-3}$, $T' \sim |t'|^{-2.5}$. The upper scale is the expansion factor.

By way of numerical solution of the system of equations (5), the evolution of the system of particles in time was calculated, the coordinates and velocity at the initial moment were chosen according to the solution (6–8). Before the moment of focusing the motion of particles in the numerical experiment can be compared with the analytical solution (6–8) to check up the accuracy of the simulation; after the focusing the accuracy of the simulation is controlled by how the Irvine–Dmitriev theorem is matched (see Section 2). Some of the results are given in Figs 1–6.

As follows from equations (6–8), both the kinetic and potential energy of the system before particles focusing increase proportionally with $(t')^{-6} \sim a^3$, $[a \sim (1+z)^{-1}]$. This ratio is valid for the numerical calculations before the focusing, according to Fig. 1. After it both values grow somewhat slower (Fig. 1). It can be mentioned that the kinetic-to-potential energy ratio which was 2/3 before focusing decreases to become 0.25 by the end of the evolutionary stage (Fig. 2).

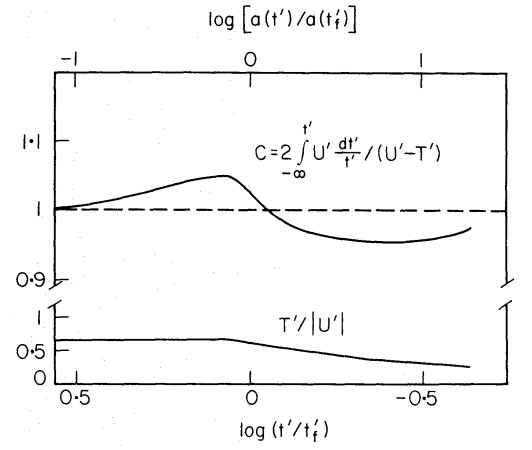

Figure 2. Dependence of the ratio of the kinetic to potential energy in the numerical experiment (low curve) and the function characterizing the accuracy of the Irvine–Dmitriev theorem being valid during time. The upper scale is the expansion factor.

During the entire stage of the evolution of the system for which calculations were made it was checked whether the Irvine–Dmitriev theorem was valid. Fig. 2 also gives the time dependence of:

$$C = 2\int_{-\infty}^{t'} U' \frac{dt'}{t'} \Big/ (U' - T'). \tag{12}$$

It can be seen here that the calculation accuracy is not worse than 5 per cent.

The evolution of the one-dimensional system is conveniently seen in the phase plane $v_1' - x_1'$ and in the plane $q_1 - x_1'$. Fig. 3 shows the system state for four moments of time $t_1' < t_f'$, $t_2' \approx t_f'$, $t_3' > t_f'$ and $t_4' > t_3'$ obtained as a result of the numerical calculations. Fig. 3 also gives the dependence of the density $\rho'(x_1')$.

Before focusing with $t' < t_f'$ the functions $v_1'(x_1')$ and $q_1(x_1')$ are in one-to-one correspondence and the inhomogeneities of the density are comparatively small. At the instant of focusing $t' = t_f'$ the derivatives $\partial v_1'/\partial x_1'$ and $\partial q_1/\partial x_1'$ go to infinity in accordance with the theory. The density must also go to infinity but in the numerical calculation it is of course finite. After the instance when particles are focused in the plane $q_1 = \pi$, as a result of their next flight, a layer forms inside of where complicated multistream motions appear (at $t_3' > t_f'$ and at $t_4' > t_3' > t_f'$). The initial stage of the evolution of systems of such a type have already been discussed (Grishuk 1966; Zeldovich 1970; Sunyaev & Zeldovich 1972; Zeldovich & Novikov 1975; Shukurov 1979) and in particular, the authors have noted that a three-stream distribution of particles appeared in the thin layer in the vicinity of the $q_1 = \pi$ point.

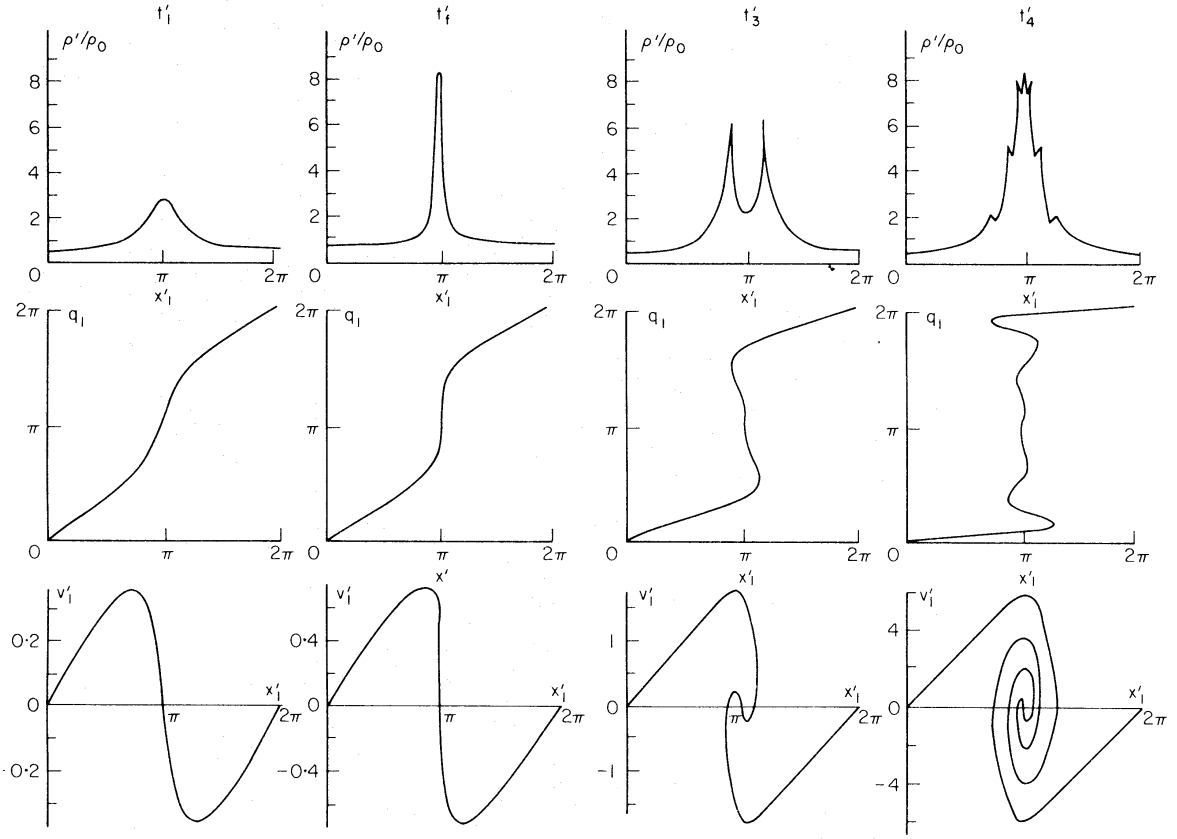

Figure 2. The system state on the phase plane $v_1' - x_1'$, on the plane $q_1 - x_1'$ and the dependence $\rho'(x_1')$ at four moments of time $t_1' < t_f' < t_3' < t_4'$. It is seen the transition of the one-flow motion with $t' = t_1'$ into the three-flow one with $t' = t_3'$ and then into the multi-flow motion with $t' = t_4'$. With $t' = t_4'$ the seven-flow distribution is observed.

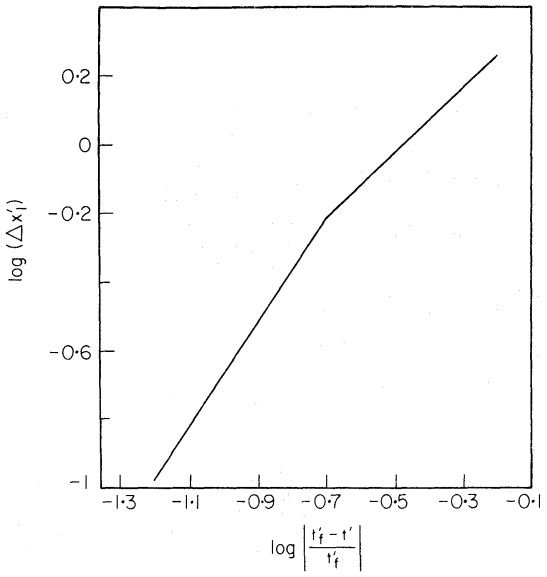

Figure 4. Time dependence of the contracted matter layer thickness. The external point where $\partial x_1'/\partial q_1 = 0$ is chosen as layer boundaries.

The instant $t_3' > t_f'$ corresponds to this situation. In this case the density must go to infinity at two points. But in the numerical calculation the density is considered to be finite and only two sharp maxima can be seen.

The numerical simulation of this problem allowed interesting data to be obtained about the evolution of this layer structure at the later stage when the analytic estimates are not true. The further complication of the configuration is the specific pecularity of the problem; there appeared three, five and more streams, the density goes to infinity not only at the layer boundaries but also at one, two and more points in the middle part of the layer. During the calculation we succeeded in detecting the appearance of nine flows and seven singularities in the density of particles (Fig. 3, at $t_4' > t_f'$). It can be shown that during subsequent evolution the number of flows will increase.

Fig. 4 represents the time dependence of the thickness of the layer. The external point with $\partial x_1'/\partial q_1 = 0$ is taken to be the layer boundary. According to the estimates obtained using the formal extension of the analytic solution (6–8), after the focusing instant t_f' (when the solution itself is not true) the layer thickness grows with time for $1 - t'/t_f' \ll 1$ as

$$\Delta x_1' = \frac{1}{12}(\Delta q)^3 \approx \frac{16}{3}(1 - t'/t_f')^{3/2}. \tag{13}$$

The numerical calculation shows that later on the growth rate becomes slower and

$$\Delta x_1' \approx 2.4(1 - t'/t_f') \tag{14}$$

(see Fig. 4) and here the transition from the law (13) to the law (14) occurs with $t' \approx 0.8t_f'$, i.e. soon after the focusing instant, and at this time $\Delta x_1' \approx 0.48$. Since the values $\Delta x_1'$, $1 - t'/t_f'$ are rather small we can assume that the transition from the law (13) to the law (14) is not associated with the specific selection of the dependence $s_1(q_1)$ in equations (6–8), but with growth of gravitational interaction, that is confirmed by the ratio T'/U' becoming smaller with time (Fig. 2). The validity of equation (14) at the end of the interval of time considered can depend on the specific selection of the $s_1(q_1)$ function type.

If the approximate theory is applied formally after focusing, the contracted layer thickness grows unlimitedly, not slower than obeying the law $\Delta x'_1 \sim (t'/t'_f)^{-2}$ (the exact form of the dependence depends on the selection of the displacement $s_1(q_1)$). In the numerical experiment the growth occurs much more slowly, and the contracted layer thickness will be finite even with $t' \to 0$ (infinite physical time). This fact must be taken into account while comparing the results of the calculation of the two- and three-dimensional problems with those obtained using the approximate theory.

It is interesting to find out the effect of particle contraction along the x'_1 axis upon the possible motion along orthogonal directions. The problems of such a type usually arise in analysing the real two- and three-dimensional pictures of the evolution, since the contraction always takes place mainly along one axis whereas the contraction along the second and third axes delays significantly. This problem is already no longer one-dimensional but we will discuss it in this section dealing with the one-dimensional problem since we assume that the initial amplitudes of displacements and velocities along the x'_2 axis are essentially smaller than along the x'_1 axis.

As it is known (Lifshitz & Khalatnikov 1963) as long as perturbations are small and the linear theory is true; any perturbations are linearly independent and must develop obeying the laws (6, 7). When these perturbations (or some of them) become larger the differences from the linear theory begin to manifest themselves.

In the numerical experiment, we initiated the calculations when the perturbation amplitude along the x'_1-axis was equal to $A_1 \approx 0.1$. Along the x'_2-axis, only the increasing mode was also chosen as an initial perturbation and the solution at the linear stage corresponds to (6, 7) with the substitution of index 1 into 2. The profile function of initial displacements was taken as $s_2(q_2) = -A_2 \sin q_2$. The amplitude A_2 was also chosen different: $A_2/A_1 = 0.1; 0.01$.

In all cases the numerical analysis of the evolution during the time of perturbation in the direction orthogonal to principal one showed that before the focusing time the interaction

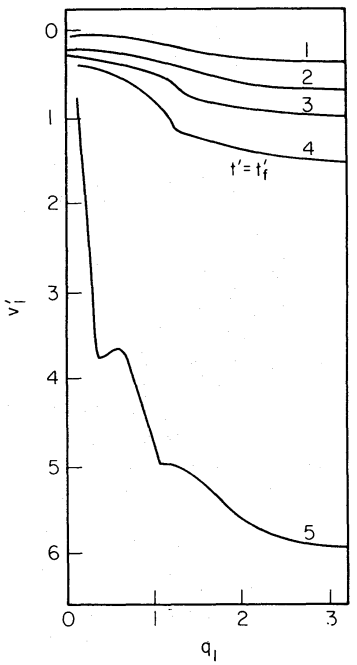

Figure 5. Distribution of the velocity profile v'_2 with time. Three upper curves correspond to the time moments $t' < t'_f$, the fourth curve to $t' \approx t'_f$ and the fifth curve to the moment of the end of calculations. The scale of the fifth curve is 10^2 times higher than the upper curves.

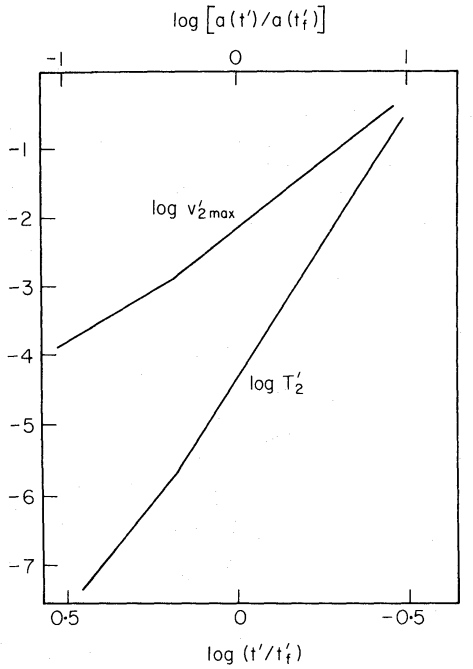

Figure 6. Time dependence of the velocity amplitude v_2' and kinetic energy of the motion along x_2': $T_2' = \frac{1}{2} \Sigma v_2'^2$.

of the flows oriented along the axes x_1 and x_2' is not essential and the inhomogeneities grow according to (6, 7). However, after the focusing along the x_1'-axis the significant inhomogeneity of density so formed results in disturbing the profile of the flow towards the x_2'-axis. In the vicinity of the point $q_1 = \pi$ inhomogeneity of velocity v_2' develops noticeably more rapidly than in the vicinity of the points $q_1 = 0$; $q_1 = 2\pi$. This is reflected by Fig. 5. Fig. 6 shows the time increase of kinetic energy $T_2' = \frac{1}{2} \Sigma v_2'^2$ as well as the velocity amplitude at the point $x_1' = \pi$, where as it follows from Fig. 5 the contraction rate is maximum. The comparison of the curves $T_2'(t')$ and $v_{2\max}'(t')$ shows that contribution from the vicinity of the points $x_1' = 0; 2\pi$ into the energy is small and these dependences are substantially identical. The multi-stream distribution of particles over the velocity after focusing suggests the posibility of the beam instability development. However, the discussed results do not predict with certainty the possible influence of the beam instability. The exponent change in the law of the dependence $v_2' \sim t'^n$ from $n = 3$ before the focusing to $n = 3.75$ after the focusing can be associated with the sharply increased inhomogeneity in the matter distribution over the x_1' axis but not with the appearance of particle beams. The obvious non-stationary state of the particle distribution over v_1' also smears the picture of the instability development. The question needs further analysis. Nevertheless the important qualitative conclusion can be made: the dependence of the rate of the inhomogeneity development in the direction of the x_2'-axis from x_1'-coordinate of the point, the more rapid development of the inhomogeneities in the vicinity of the focusing point and the delay of the periphery, is not related to the assumptions used in the calculations and can be essential in the evolution of the inhomogeneities in the general case.

Thus the analysis of the results of the numerical calculation of the one-dimensional problem allows the following conclusions to be made: 1. After focusing the particles are oscillating in the thin layer about the plane of focusing, the thickness of which is slowly increasing with time. The particle oscillation amplitude is the higher the later these particles

have been focused. 2. Focusing of particles and the further formation of the large inhomogeneities in the plane strongly affects the evolution of inhomogeneities accelerating the gravitational contraction and disturbing the perturbation profile.

4 Two-dimensional numerical simulation of the gravitational instability process

This section deals with some results of the two-dimensional numerical experiment simulating the process of the large-scale structure formation in the Universe and compares the results of the numerical calculations of the approximate theory. Note that in the two-dimensional problem there appear qualitatively the basic features of the real three-dimensional case.

The two-dimensional numerical experiment consists in solving equations (3) for the system with 4096 particles of the same mass interacting with the force $F \sim 1/z$ with the periodical boundary conditions. The random perturbations of both the density and the velocity were chosen as the initial data with the definite correlation function. Only long-wave perturbations were taken as the initial conditions, $2\pi \geqslant \lambda \geqslant 2\pi/9$, (the size of the square is equal to 2π), λ is a wavelength of perturbations.

The numerical simulation started from the moment when the typical amplitude of the density perturbations was small, $\delta\rho/\rho \approx 0.1$ the initial perturbations (see Section 3) were given by the function:

$$\mathbf{s}(\mathbf{q}) = \sum_{i=0}^{9} \sum_{j=0}^{9} \frac{\mathbf{k}_{ij}}{k_{ij}^2} (A_{ij} \cos \mathbf{k}_{ij}\mathbf{q} + B_{ij} \sin \mathbf{k}_{ij}\mathbf{q})$$
$$\mathbf{k}_{ij} = (i, j) \qquad (15)$$

A_{ij} and B_{ij} are random numbers distributed according to the normal law with unit dispersion and zero mean. The chosen perturbations have the 'flat' spectrum of density perturbations in the range from $\lambda \approx 2\pi/9$ up to $\lambda = 2\pi$. The cut-off of the spectrum at short waves modulates the adiabatic initial conditions and determines the formation of cellular structure in the non-linear stage.

The evolution of the same initial distribution of perturbations was also calculated using the approximate theory and both results were compared.

This comparison basically confirms the most important qualitative conclusions of the approximate theory: at the first stage of the evolution of the system of gravitationally interacting points some thin very-extended clusters are formed. These clusters then disintegrate into the parts and gather into several conglomerates. It is evident that the last stage is not described any longer by the approximate theory.

Fig. 7 gives the two-dimensional distributions of particles obtained (a) according to the approximate theory and (b) as a result of the numerical experiment. In both cases the initial conditions were identical and the distribution of points given for the same time.

In comparing the two figures the similarity of the distributions is obvious, though there are some significant discrepancies. We also note not only the extended one-dimensional structures typical of both pictures predominate but also many details of location and shape of the regions with higher and lower density seem to be identical. At the same time it should be noted that the picture obtained in the numerical experiment is more contrasted, the regions with the increased density are more distinct, the compact clusters are seen in the intersections of the linear structures. Above all, it is associated with the effect (pointed out in Section 3) of smearing the layer with the higher density after focusing in the approximate theory. As the analysis made in Section 3, and the two-dimensional model in Fig. 7, shows that the regions with the higher density formed under the real conditions are expanding very slowly; and the motion of particles along the linear formations naturally results in the

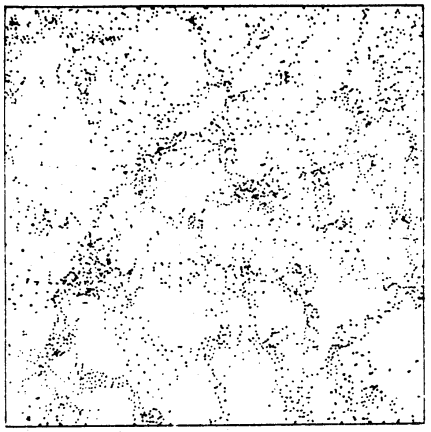

(a)

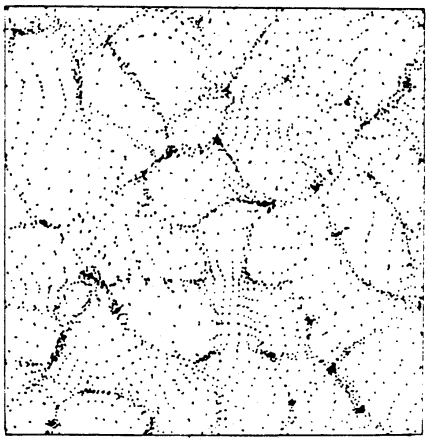

(b)

Figure 7. Two-dimensional distribution of particles obtained from (a) the approximate theory and (b) the numerical simulation ($\Omega = 1$), $t' = 0.66t'_c$. At $t' = t'_c\langle(\delta\rho/\rho)^2\rangle^{1/2}$ calculated according with linear theory is equal to 1; $a/a(t'_c) = 2.3$.

compact clusters appearing at the points of the cellular structure. It is possibly the regions where the rich clusters of galaxies can be formed.

The typical cellular structure, when the most part of matter is gathered in thin layers dividing vast low-density regions, forms at the non-linear stage in $\delta\rho/\rho$. However, it is clear that the above distribution of self-gravitating particles is too far from equilibrium, so that the structure only exists for a finite time. The numerical experiments show that it fragments into compact objects; these merge in more massive objects (Figs 8 and 9). The observable concentration of particles in the bottom of the picture (Fig. 9) is connected with the existence of long-wave perturbations ($\lambda \approx 2\pi$) in the initial distribution.

Another picture is seen in the open models ($\Omega < 1$). It is known that in this case the growth of perturbations is frozen, therefore it is possible that, after formation, the large-scale cellular structure exists forever, as evolution on a small scale continues.

The qualitative comparison of the approximate theory with the results of the numerical simulation was carried out by comparing the trajectories for several randomly chosen particles and averaging over all the particles considered. The values were calculated

$$g_x^2 = \frac{(x'_1 - x_1^*)^2 + (x'_2 - x_2^*)^2}{(x'_1 - x'_{10})^2 + (x'_2 - x'_{20})^2} \tag{16}$$

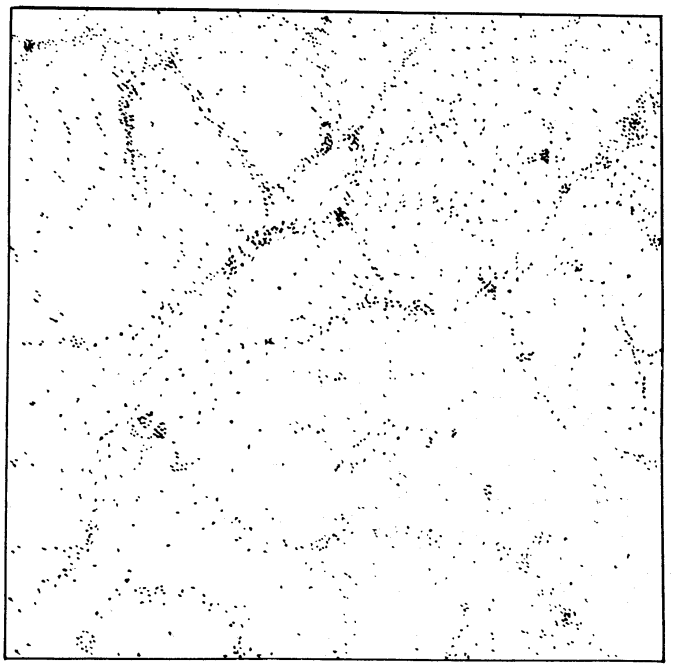

Figure 8. Distribution of particles corresponds to Fig. 7 but it is taken at later time ($\Omega = 1$). $t' = 0.49 t'_c$, $a/a(t'_c) = 4.2$.

where x'_i and x'_{i0} are the current and initial coordinates of a particle in the numerical experiment; x_i^* is current coordinate of a particle according to the approximate theory. Fig. 10 gives dependences g_x for three particles chosen by chance and the value of the deflection $\langle g_x^2 \rangle^{1/2}$ averaged over all the particles. Fig. 12 shows similar dependences of relative deflections of velocity in the numerical experiment of the approximate theory for the three

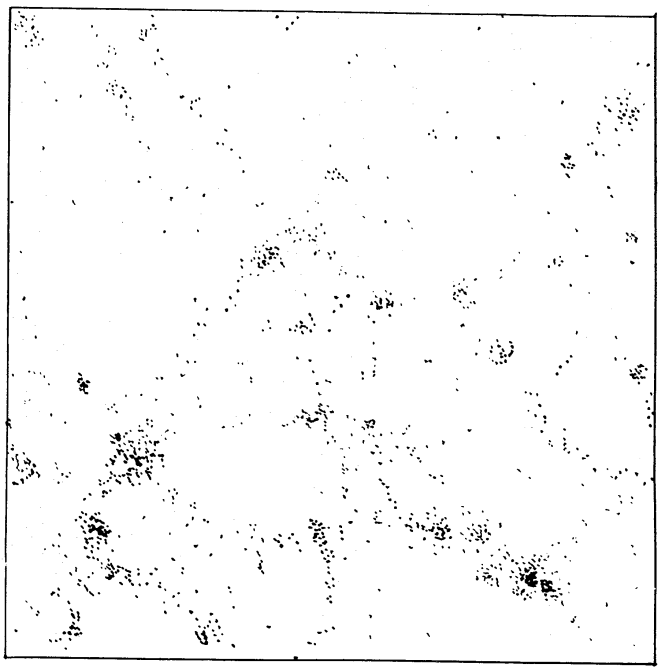

Figure 9. The same as Fig. 7 but the time is later than in Fig. 8, ($\Omega = 1$). $t' = 0.37 t'_c$, $a/a(t'_c) = 7.4$.

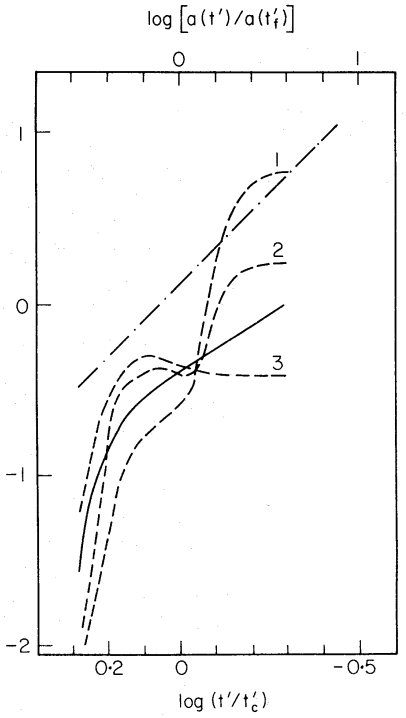

Figure 10. Dependence of logarithm of $g_x(t')$ for three single particles (dashed line) and $\langle g_x^2\rangle^{1/2}$ (solid line). To compare the dependence of the logarithm of density perturbations log $\langle(\delta\rho/\rho)^2\rangle^{1/2}$ on time is given according to the linear theory (dash–dot line). At $t' = t'_c$, $\langle(\delta\rho/\rho)^2\rangle^{1/2}$ calculated according to the linear theory is equal to 1.

particles

$$g_v^2 = \frac{(v_1' - v_1^*)^2 + (v_2' - v_2^*)^2}{(v_1' - v_{10}')^2 + (v_2' - v_{20}')^2}. \tag{17}$$

Here v_i' and v_{i0}' are the current and initial values of particle velocity in the numerical exeriment; v_i^* is the particle velocity according to the approximate theory; and $\langle g_v^2\rangle^{1/2}$ is the velocity deflection averaged over all particles. Figs 10 and 11 show that the small (at the beginning) discrepancies increase with time and that the errors in the approximate theory for the determination of position and velocity of a single particle also become significant for an average over all the particles. However, comparison with the curve $\langle(\delta\rho/\rho)^2\rangle^{1/2}$ in Fig. 12 shows that the approximate theory is valid up to the values $\langle(\delta\rho/\rho)^2\rangle^{1/2} \approx 2$–3, when not less than 70 per cent of the matter is contained in the contracted phase. Since the approximate theory describes only the matter motion before focusing, the increase of discrepancy between the approximate theory and the numerical experiment at this period is not surprising. As it has been shown while analysing the one-dimensional problem, equations (3) lead to oscillations of particles after focusing within the thin layer whereas according to the approximate theory both the velocity of a particle and its displacement increase unlimitedly before and after focusing. The growth of discrepancies occurs as much in the single particle as for the averaged curve. The errors in the velocities (Fig. 9) accumulate somewhat faster than the errors in coordinates, since the coordinates of particles are determined by integration of their velocities.

Fig. 12 gives the time dependence of the density perturbations $\langle(\delta\rho/\rho)^2\rangle^{1/2}$ according to the linear theory and the results of numerical calculations. It is interesting to note that the

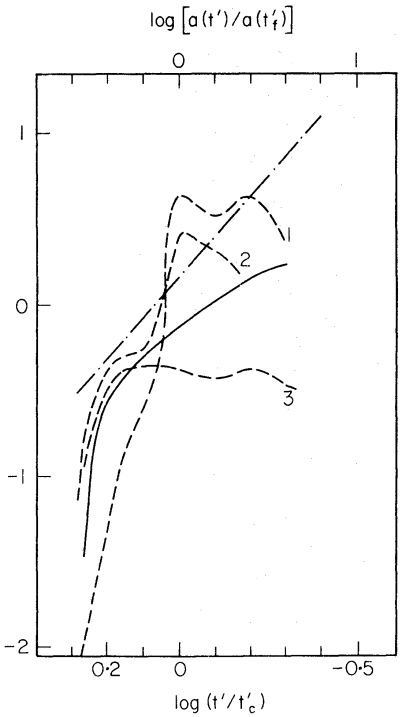

Figure 11. Dependence of the logarithm of $g_v(t')$ for three single particles (dashed line) and $\langle g_v^2 \rangle^{1/2}$ (solid line), log $\langle(\delta\rho/\rho)^2\rangle^{1/2}$ according to the linear theory – dash-dot line.

linear dependence accurately describes the dependence $\langle(\delta\rho/\rho)^2\rangle^{1/2}$ on time up to the value $\langle(\delta\rho/\rho)^2\rangle^{1/2} \approx 2.5$. However, it does not mean of course that the linear theory as a whole is applicable up to such a stage, even the qualitative conclusions of the linear theory are not strictly true at this period. At the later stages of evolution, when almost all the matter has already been converted into the contents of condensations, the growth of perturbations

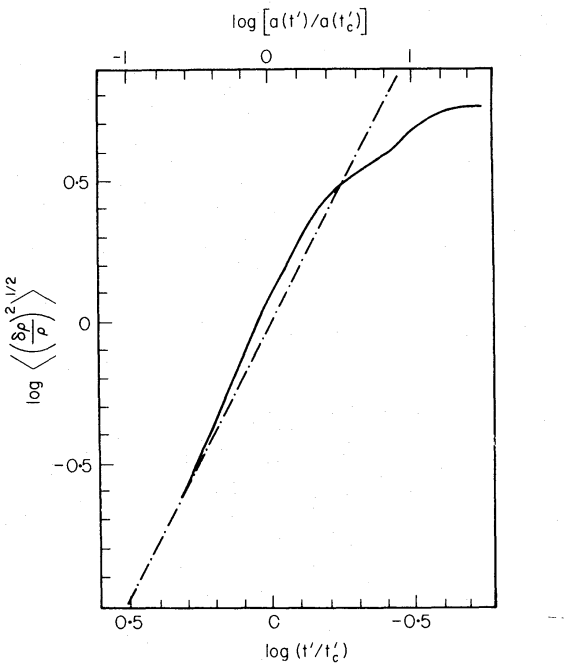

Figure 12. Dependence of $\langle(\delta\rho/\rho)^2\rangle^{1/2}$ obtained from the numerical experiment (solid line) and according to the linear theory (dash-dot line).

becomes sharply slower. Ar this stage the clustering of the matter inside 'pancakes' occurs and the linear theory is evidently not applicable.

Note that the Irvine–Dmitriev theorem is satisfied with an accuracy up to 10–15 per cent that is characteristic of the calculation accuracy.

Now we shortly formulate the main results of the numerical simulations.

1. If the spectrum of initial perturbations does not keep waves with lengths of the order of the mean distance between particles then the cellular structure does form in the non-linear stage. The mean scale of the cellular structure is about the shortest wave, keeping in the spectrum of the initial perturbations.

2. In the case of the Robertson–Walker model $\Omega = 1$, the cellular structure exists for a finite time and then it disappears. In the open models of the Universe with a definite choice of the amplitude of initial perturbations, the cellular structure can freeze and exist forever.

3. The cellular structure forms not only in the hydrodynamic system but in the collisionless system too. In the two-dimensional case under consideration the gravitational force is enough to hold the structure formed by intersection such that it will not disappear soon after the time of formation but exist for a finite time.

4. The comparison of the results of numerical experiments in the two-dimensional case with the approximate theory of gravitational instability gives arguments in favour of the correctness of the qualitative results in the three-dimensional case too.

References

Birdsull, C. K. & Fuss, D., 1969. *J. comput. Phys.*, **3**, 4941.
Dmitriev, N. A. & Zeldovich, Ya. B., 1963. *Zh. eksp. teor. Fiz.*, **45**, 1150.
Dmitriev, N. A. & Zeldovich, Ya. B., 1964. *Zh. eksp. teor. Fiz.*, **48**, 79.
Doroshkevich, A. G., Ryabenki, V. S. & Shandarin, S. F., 1973. *Astrofizica*, **9**, 257.
Doroshkevich, A. G. & Sandarin, S. F., 1973. *Astrofizica*, **9**, 549.
Fedorenko, R. P., 1973. *Usp. mat. Nauk*, **XXVIII**, 121.
Grishuk, L. P., 1966. *Zh. eksp. teor. Fiz.*, **51**, 475.
Hockney, J. W., 1970. *Math. comput. Phys.*, No. 9, Academic Press, New York.
Irvine, W. M., 1961. *Doctoral thesis*, Harvard University.
Kadomzev, B. B., 1976. *The Collective Effects in Plasma*, Nauka, Moscow.
Kotok, E. V. & Sigov, Yu. S., 1970. *The report at VII Int. Symp. on Dynamics of Rarefied Gas*, Italy.
Lifshitz, E. M., 1946. *Zh. eksp. teor. Fiz.*, **16**, 587.
Lifshitz, E. M. & Khalatnikov, I. M., 1963. *Usp. fiz. Nauk*, **80**, 391.
Novikov, I. D., 1975. *Astr. Zh.*, **52**, 1038.
Polyachenko, V. L. & Friedman, A. M., 1976. *The Equilibrium and Stability of Gravitating Systems*, Nauka, Moscow.
Poludov, A. M., Sagdeev, R. Z. & Sigov, Yu. S., 1974. Preprint IAM, No. 129.
Samarski, A. A., 1971. *The Introduction in the Theory of Difference Schemes.*
Shukurov, A. M., 1979. *Astrofizica*, in press.
Sunyaev, R. A. & Zeldovich, Ya. B., 1972. *Astr. Astrophys.*, **20**, 189.
Zeldovich, Ya. B., 1970. *Astrofizica*, **6**, 119, *Astr. Astrophys.*, **5**, 84.
Zeldovich, Ya. B. & Novikov, I. D., 1975. *Structure and Evolution of the Universe*, Moscow.